

Ringed accretion disks: instabilities

D. Pugliese and Z. Stuchlík

Institute of Physics and Research Centre of Theoretical Physics and Astrophysics, Faculty of Philosophy & Science, Silesian University in Opava, Bezručovo náměstí 13, CZ-74601 Opava, Czech Republic

d.pugliese.physics@gmail.com;zdenek.stuchlik@physics.cz

ABSTRACT

We analyze the possibility that several instability points may be formed, due to the Paczyński mechanism of violation of mechanical equilibrium, in the orbiting matter around a supermassive Kerr black hole. We consider recently proposed model of ringed accretion disk, made up by several tori (rings) which can be corotating or counterrotating relative to the Kerr attractor due to the history of the accretion process. Each torus is governed by the general relativistic hydrodynamic Boyer condition of equilibrium configurations of rotating perfect fluids. We prove that the number of the instability points is generally limited and depends on the dimensionless spin of the rotating attractor.

Subject headings: Accretion disks, accretion, jets, black hole physics, hydrodynamics

1. Introduction

The physics of accretion disks around very compact objects as supermassive black holes (BH) in active galactic nuclei (AGN) or quasars is the basis of the phenomenology of the high energy astrophysics. The instability phases of the orbiting toroidal configurations are particularly relevant during the accretion phase onto the black hole and launching of jets of matter and radiation. On one side an important issue is description of the mechanisms by which jets are launched and formed, on the other side, the relation between material in accretion and the jet power has to be clarified.

An important subject of investigation concerns the dynamics of the entire black hole-disk system, which could also result in processes producing instability of the entire system. It is often assumed that the rotational energy of the attractor may have a role in the energy extraction and conversion of matter in jet-like structures, when the gravitational binding energy of accreting matter is transformed into radiation. An intriguing issue consists in significance of the gravo-hydrostatic contribution to the jet formation and structure. Existence of a possible jet-accretion correlation itself is subject of many theoretical and observational investigation. Various analysis suggest that a significant part of matter going through the accretion point would possibly power or feed the launching jets. Therefore, we could actually consider an accretion-ejection engine by referring the accretion disk being connected to the relativistic jets.

The quest of a jet-accretion correlation for the formation and feeding of jets, or also the morphological deformation of the matter funnels would provide several constraints for any model of accretion and jet formation, depending also on the dimensionless spin of the black hole. In fact, the jet formation appears to be strongly related to the intrinsic rotation of the central attractor Lovelace et al. (2014). The role of spin and magnetic field in accretion disks and relativistic jets is discussed for example in McKinney et al. (2013) while the relation between accretion rate and jet power in x-ray luminous elliptical galaxies has been exploited in Allen et al. (2006). Creation of jets by accretion disks orbiting magnetized black holes has been recently proposed in Stuchlík&Kolos (2016).

The observational evidences for an accretion-disk origin for a radio jet in an active galaxy is discussed in Marscher et al. (2002). For the jet-disk connection and blazar unification see (Maraschi&Tavecchio 2003;

Chen et al. 2015; Yu et al. 2015; Zhang et al. 2015). For the the disk-jet connection in AGN see Sbarrato et al. (2014) and Coughlin&Begelman (2014). For the stellar BH case for example Maitra et al. (2009) and Fender&Munoz-Darias (2015).

Jets from geometrically thick disk were studied in (Abramowicz&Sharp 1983; Sadowski&Narayan 2015; Okuda et al. 2005; Ferreira&Casse 2004; Lyutikov 2009). Theoretical models for the production of relativistic jets of active galactic nuclei predict that jet power is governed by the spin and mass of the central super-massive black hole, as well as by the magnetic field near the event horizon Ghisellini et al. (2014), while no correlation between disk height and jet power appears in GR-MHD simulations presented in Fragile et al. (2012). Focusing on the general problem of the role of the accretion disk-jet connection one can question if any changes in the inner part of the disk should produce changes in the jet launching. For example Miller et al. (2012) suggest that the jet is not affected by changes in the inner radius of the accretion disk, but it depends on some of the disk properties, as its flux, temperature, and ionization. Further open question is the role of the inner margin of the accretion disk in the jet processes, namely the role of the marginally stable circular orbit (ISCO), as the definition of the inner margin of the accretion disk is extensively debated (Krolik&Hawley 2002; Bromley et al. 1998; Abramowicz et al. 2010; Agol&Krolik 2000; Paczyński 2000). Some results lead to the conclusions that a standard thin accretion disk that extends to the ISCO can drive relativistic jets Miller et al. (2012).

In the present article we consider the emergence of several instability points in a ringed disk Pugliese&Stuchlík (2015). The instability points can be associated to accretion into the black hole, or irregular points of critical surfaces representing open structures of matter funnels, the proto-jets (Kozłowski et al. 1978; Abramowicz et al. 1978; Sadowski et al. 2015; Lasota et al. 2015; Lyutikov 2009; Madau 1988; Sikora 1981; Stuchlík et al. 2009, 2015; Slaný&Stuchlík 2005; Stuchlík 2005). We study different kinds of gravo-hydrostatic instability points assuming the hydrostatic pressure and gravitational effects of a Kerr black hole background requiring a full general relativistic treatment of geometrically thick accretion disks. We realize the analysis in the framework of the ringed accretion disks (or macro-structures) recently introduced in Pugliese&Stuchlík (2015). The ringed accretion disk model is made up by several rings rotating around a super massive Kerr black hole attractor which could be created in various regimes during the evolution of matter configurations around supermassive black holes. We start by the consideration that different parts of the orbiting material around a super-massive spinning black hole, characterized by different specific angular momentum, may give rise to instability in different points, inducing eventually an overall instability of the entire ringed orbiting structure.

In modelling the evolution of supermassive black holes in AGNs both corotating and counter-rotating accretion stages are mixed (Volonteri et al. 2003a; Carmona-Loaiza et al. 2015; Dyda et al. 2015; Hohlfeld&Lovelace 2014). Therefore, the galactic nuclei containing a supermassive black hole could be an environment where these macro-structure can be observed. Toroidal rings might be formed as remnants of several accretion regimes occurred in various phases of the black hole life Alig et al. (2013); King&Pringle (2007, 2006); Lovelace&Chou (1996); Gafton et al. (2015). These sub-structures could be eventually reanimated in non isolated systems where the central attractor is interacting with the environment, or in some kinds of binary systems. Some additional matter, for example, could be supplied into the vicinity of the central black hole due to tidal distortion of a star Miller et al. (2015). Possible observational evidences of these configurations were also discussed in (Karas&Sochora 2010; Sochora et al. 2011), more generally a possible evidence of the existence of the ringed accretion disk can be inferred from the study of the optical properties of the disk (Stuchlík&Schee 2012, 2010).

The individual toroidal (thick disk) configurations (the rings or sub-configurations) are here described by the purely hydrodynamic (barotropic) model. The Polish Doughnut (P-D) model Abramowicz&Fragile (2013) is an example of a thick, opaque and super-Eddington, radiation pressure supported accretion disks cooled by advection with low viscosity Abramowicz et al. (1983). Each toroid of the ringed disk is assumed being governed by the General Relativity hydrodynamic Boyer condition of equilibrium configurations of rotating perfect fluids. The effects of strong gravitational fields are dominant with respect to the dissipative ones and predominant to determine the unstable phases of the system (Font&Daigne 2002b; Igumenshchev

2000; Abramowicz&Fragile 2013; Pugliese&Montani 2015; Paczyński 1980), where the entropy is constant along the flow. The von Zeipel condition is verified and accordingly the surfaces of constant angular velocity Ω and of constant specific angular momentum ℓ coincide (Abramowicz 1971; Chakrabarti 1990, 1991; Zanotti&Pugliese 2014) and the rotation law $\ell = \ell(\Omega)$ is independent of the equation of state (Lei et al. 2008; Abramowicz 2008; Abramowicz et al. 1978). Properties of each tori can be then determined by an effective potential reflecting the background Kerr geometry. The equipotential surfaces associated with critical points identify the toroidal surfaces of the disk. The cusped surfaces are the critical topologies associated to the unstable phases of the configurations. The outflow of matter through the cusp occurs by the Paczyński-Wiita (P-W) mechanism of violation of mechanical equilibrium of the tori, i.e. an instability in the balance of the gravitational and inertial forces and the pressure gradients in the fluid (Abramowicz&Fragile (2013)).

As in Pugliese&Stuchlík (2015) we consider the ringed disk where the centers of all the individual tori are coplanar, coinciding with the equatorial plane of the Kerr attractor. This assumption of coincidence between the orbital planes of the rings and the equatorial plane of the axisymmetric attractor, is the simplest scenario for the majority of the current analytical and numerical models of the extended accreting matter¹. We face particularly the problem of location of the inner and outer edges of the toroidal configurations and the critical points with respect to the marginally bounded and marginally stable circular orbits. This analysis provides the basis for the attractor classifications. The rings are related by boundary conditions dictated by the condition of not penetration of matter and by the geometric constraint for the equilibrium configurations determined by the geometric properties of the Kerr background reflected by its geodesic structure. The condition of non-penetration of matter was considered in Pugliese&Stuchlík (2015) in a very restrictive way, avoiding collisions in the macro-structure. As a consequence of this assumption only a point of instability would be possible in the macro-configuration. In the present article we weaken this request, investigating the possibility that there may be several P-W points for a given macro-configuration. We distinguish five types of unstable couples of orbiting configurations (*states* of the macro-configurations). Not all these states can actually exist. We prove that their formation and stability depends on the dimensionless spin of the attractor, the relative rotation of the tori with respect to the attractor, and more importantly, the relative rotation of the fluids in the ringed disk. Considering the possible combination of these states, we investigate also ringed disks consisting of more than two rings and a possible state correlation occurring when two surfaces are in contact leading to collision phenomena and eventually to a topological transition of the state and, consequently, of the entire macro-configuration. We face the problem of the state evolution considering the condition for an initial couple of configurations (starting state) could evolve towards a transition of the surface topologies with emergence of instability.

This article is structured as follows: in the first brief descriptive part, Sec. (2) the ringed disk model is introduced and some general considerations on the instability points are discussed. Sec. (3) addresses briefly the main outcomes of the analysis focusing on the states properties, details will be provided in future studies. Concluding remarks can be found in Sec. (4).

2. Rings in the Kerr spacetime

In this section, we introduce the main notation used in this work and we will make reference also to some basic notions introduced in Pugliese&Stuchlík (2015). The Kerr metric tensor in the Boyer-Lindquist (BL) coordinates $\{t, r, \theta, \phi\}$ reads

$$ds^2 = -dt^2 + \frac{\rho^2}{\Delta} dr^2 + \rho^2 d\theta^2 + (r^2 + a^2) \sin^2 \theta d\phi^2 + \frac{2M}{\rho^2} r (dt - a \sin^2 \theta d\phi)^2, \quad (1)$$

where $\rho^2 \equiv r^2 + a^2 \cos^2 \theta$ and $\Delta \equiv r^2 - 2Mr + a^2$,

¹Off-equatorial configurations are considered in (Kovar et al. 2008; Cremaschini et al. 2013) and in (Dogan et al. 2015; Nixon&King 2012; Nixon et al. 2012a,b, 2013; Dunhill et al. 2014; Nixon et al. 2011) where also strongly misaligned disks with respect to the central supermassive BH spin are considered.

where the specific angular momentum is $a = J/M \in]0, 1]$, M is a mass parameter and J is the total angular momentum of the gravitational source. The extreme Kerr black hole has dimensionless spin $a/M = 1$, while the non-rotating limiting case $a = 0$ is the Schwarzschild metric². The horizons $r_- < r_+$ and the outer static limit r_ϵ^+ are respectively given by:

$$r_\pm \equiv M \pm \sqrt{M^2 - a^2}; \quad r_\epsilon^+ \equiv M + \sqrt{M^2 - a^2 \cos^2 \theta}; \quad (2)$$

where $r_+ < r_\epsilon^+$ on $\theta \neq 0$ and $r_\epsilon^+ = 2M$ in the equatorial plane $\theta = \pi/2$. We consider toroidal configurations of perfect fluids orbiting a Kerr black hole (**BH**) attractor. Importantly, the Kerr geometry has two Killing vectors: $\xi_\phi = \partial_\phi$, rotational Killing field, and $\xi_t = \partial_t$, which is the Killing field representing the stationarity of the spacetime. Line element (1) is indeed independent of ϕ and t . Consequently, the quantities

$$E \equiv -g_{\alpha\beta} \xi_t^\alpha p^\beta = -p_t, \quad L \equiv g_{\alpha\beta} \xi_\phi^\alpha p^\beta = p_\phi, \quad (3)$$

are constants of motion and p_a is the particle four-momentum. We can limit the analysis of the test particle circular motion to the case of positive values of a for corotating ($L > 0$) and counterrotating ($L < 0$) orbits with respect to the black hole. In fact the metric tensor (1) is invariant under the application of any two different transformations: $x^\alpha \rightarrow -x^\alpha$ for one of the coordinates (t, ϕ) , or the metric parameter a and, consequently, the test particle dynamics is invariant under the mutual transformation of the parameters $(a, L) \rightarrow (-a, -L)$. The constant L in Eq. (3) may be interpreted as the axial component of the angular momentum of a particle for timelike geodesics and E as representing the total energy of the test particle coming from radial infinity, as measured by a static observer at infinity. In this work we deal with a one-species particle perfect fluid system, which is described by the energy momentum tensor

$$T_{\alpha\beta} = (\varrho + p)u_\alpha u_\beta + p g_{\alpha\beta}, \quad (4)$$

where ϱ and p are the total energy density and pressure, respectively, as measured by an observer comoving with the fluid whose four-velocity u^α is a timelike flow vector field. The fluid dynamics is described by the *continuity equation* and the *Euler equation* respectively:

$$u^\alpha \nabla_\alpha \varrho + (p + \varrho) \nabla^\alpha u_\alpha = 0, \quad (p + \varrho) u^\alpha \nabla_\alpha u^\gamma + h^{\beta\gamma} \nabla_\beta p = 0, \quad (5)$$

where $\nabla_\alpha g_{\beta\gamma} = 0$ and for the symmetries of the problem, we assume $\partial_t \mathbf{Q} = 0$ and $\partial_\phi \mathbf{Q} = 0$, with \mathbf{Q} being a generic spacetime tensor. In Eq. (5), $h_{\alpha\beta} = g_{\alpha\beta} + u_\alpha u_\beta$ is the projection tensor (Pugliese&Kroon 2012; Pugliese&Montani 2015). Assuming a barotropic equation of state $p = p(\varrho)$, we investigate the fluid toroidal configurations (with $u^\theta = 0$) centered on the plane $\theta = \pi/2$, and defined by the constraint $u^r = 0$. Thus, in this setup we find from the Euler equation (5)

$$\frac{\partial_\mu p}{\varrho + p} = -\partial_\mu W + \frac{\Omega \partial_\mu \ell}{1 - \Omega \ell}, \quad \ell \equiv \frac{L}{E}, \quad W \equiv \ln V_{eff}(\ell), \quad V_{eff}(\ell) = u_t = \pm \sqrt{\frac{g_{\phi t}^2 - g_{tt} g_{\phi\phi}}{g_{\phi\phi} + 2\ell g_{\phi t} + \ell^2 g_{tt}}}, \quad (6)$$

(the continuity equation in Eq. (5) is identically satisfied as consequence of the applied conditions and symmetries). The function $V_{eff}(\ell)$ is the effective potential for the fluid, the function W is the Paczyński-Wiita (P-W) potential, reflecting the background Kerr geometry and the centrifugal effects, and we assume here a constant and conserved specific angular momentum ℓ (see also (Lei et al. 2008; Abramowicz 2008)). Finally, Ω is the relativistic angular frequency of the fluid relative to the distant observer. Similarly to the case of the test particle dynamics, the function $V_{eff}(\ell)$ in Eq. (6) is invariant under the mutual transformation of the parameters $(a, \ell) \rightarrow (-a, -\ell)$. Therefore, we can limit the analysis to positive values of $a > 0$,

²We adopt the geometrical units $c = 1 = G$ and the $(-, +, +, +)$ signature, Greek indices run in $\{0, 1, 2, 3\}$. The four-velocity satisfy $u^\alpha u_\alpha = -1$. The radius r has unit of mass $[M]$, and the angular momentum units of $[M]^2$, the velocities $[u^t] = [u^r] = 1$ and $[u^\phi] = [u^\theta] = [M]^{-1}$ with $[u^\phi/u^t] = [M]^{-1}$ and $[u_\phi/u_t] = [M]$. For the seek of convenience, we always consider the dimensionless energy and effective potential $[V_{eff}] = 1$ and an angular momentum per unit of mass $[L]/[M] = [M]$.

for *corotating* ($\ell > 0$) and *counterrotating* ($\ell < 0$) fluids and we adopt the notation (\pm) for counterrotating or corotating matter respectively. We consider a fully general relativistic model of ringed accretion disk formed by several corotating and counterrotating toroidal rings orbiting a supermassive Kerr attractor (Pugliese&Stuchlík 2015). In a given spacetime characterized by the dimensionless spin (a/M), each toroid of the ringed disk is governed by the General Relativity hydrodynamic Boyer condition of equilibrium configurations of rotating perfect fluids. According to the Boyer theory on the equipressure surfaces applied to a P-D torus, the toroidal surfaces are the equipotential surfaces of the effective potential $V_{eff}(\ell, r)$, solutions of $V_{eff} = K = \text{constant}$ or $\ln(V_{eff}) = c = \text{constant}$ (Boyer 1965; Frank et al. 2002). These correspond also to the surfaces of constant density, specific angular momentum ℓ , and constant relativistic angular frequency Ω , where $\Omega = \Omega(\ell)$ as a consequence of the von Zeipel theorem (Abramowicz 1971; Zanotti&Pugliese 2014). Each Boyer surface is uniquely identified by the couple of parameters $\mathbf{p} \equiv (\ell, K)$. Since the toroidal configuration can be corotating, $\ell a > 0$, or counterrotating, $\ell a < 0$, with respect to the black hole rotation ($a > 0$), assuming first a couple (C_a, C_b) with specific angular momentum (ℓ_a, ℓ_b) , orbiting in the equatorial plane of a given Kerr **BH**, we need to introduce the concept of ℓ corotating disks, defined by the condition $\ell_a \ell_b > 0$, and ℓ counterrotating disks defined by the relations $\ell_a \ell_b < 0$. The two ℓ corotating tori can be both corotating, $\ell a > 0$, or counterrotating, $\ell a < 0$, with respect to the central attractor. Fig. (1) represents a ringed accretion disk with equilibrium configurations and open (O_x proto-jet) surfaces. It will be important

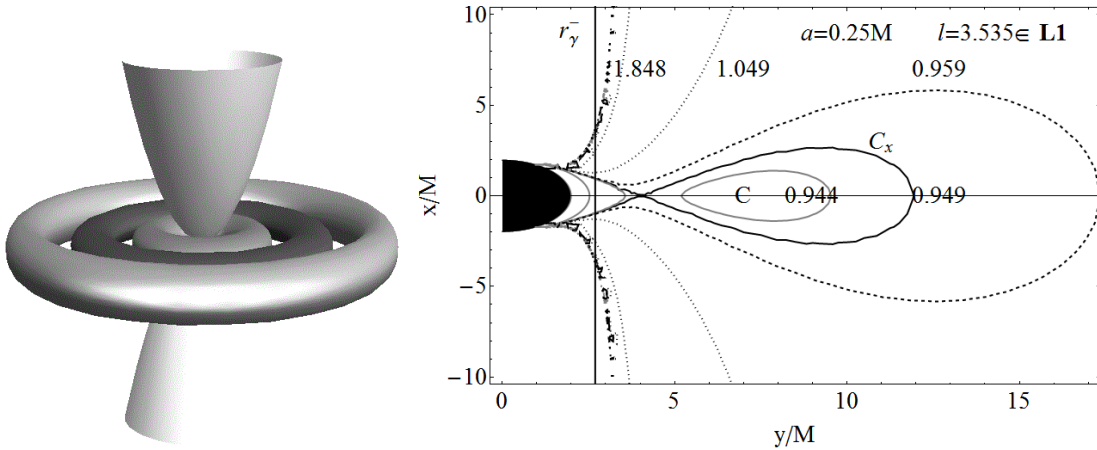


Fig. 1.— Left: Pictorial representation of a ringed accretion disk. Right: Spacetime spin $a = 0.25M$, ℓ corotating sequences, $\ell_i \ell_j > 0$, of corotating disks $\ell_i a > 0 \forall ij$. The outer horizon is at $r_+ = 1.96825M$, the region $r < r_+$ is black-colored.

to consider in the analysis of the ringed disks the notable radii $r_{\mathcal{N}}^{\pm} \equiv \{r_{\gamma}^{\pm}, r_{mbo}^{\pm}, r_{mso}^{\pm}\}$, defining the geodesic structure of the Kerr spacetime with respect to the matter distribution: a geometric property of the spacetime consisting of the union of the orbital regions with boundaries in $r_{\mathcal{N}}$ —as sketched in Fig. (2). It can be decomposed, for $a \neq 0$, into $r_{\mathcal{N}}^-$ for the corotating and $r_{\mathcal{N}}^+$ counterrotating matter. Since the intersection of $r_{\mathcal{N}}^{\pm}$ is not empty, the analysis of the geodesic structure will be particularly relevant in the characterization of the ℓ counterrotating sequences (Pugliese&Stuchlík 2015). Specifically, for timelike particle orbits, r_{γ}^{\pm} is the *marginally circular orbit* or the photon circular orbit, timelike circular orbits can fill the spacetime region $r > r_{\gamma}^{\pm}$. The *marginally stable circular orbit* r_{mso}^{\pm} : stable orbits are in $r > r_{mso}^{\pm}$ for counterrotating and corotating particles respectively. The *marginally bounded circular orbit* is r_{mbo}^{\pm} , where $E_{\pm}(r_{mbo}^{\pm}) = 1$ (Pugliese et al. 2011, 2013; Pugliese&Quevedo 2015). Given $r_i \in \mathcal{R}$, we adopt the notation for any function $\mathbf{Q}(r)$: $\mathbf{Q}_i \equiv \mathbf{Q}(r_i)$, therefore for example $\ell_{mso}^+ \equiv \ell_+(r_{mso}^+)$, and more generally given the radius r_* and the function $\mathbf{Q}(r)$, there is $\mathbf{Q}_* \equiv \mathbf{Q}(r_*)$. We focus on the solution of Eq. (6), $W = \text{constant}$, associated to the critical points of the effective potential, with constant angular momentum and parameter K . Thus, we con-

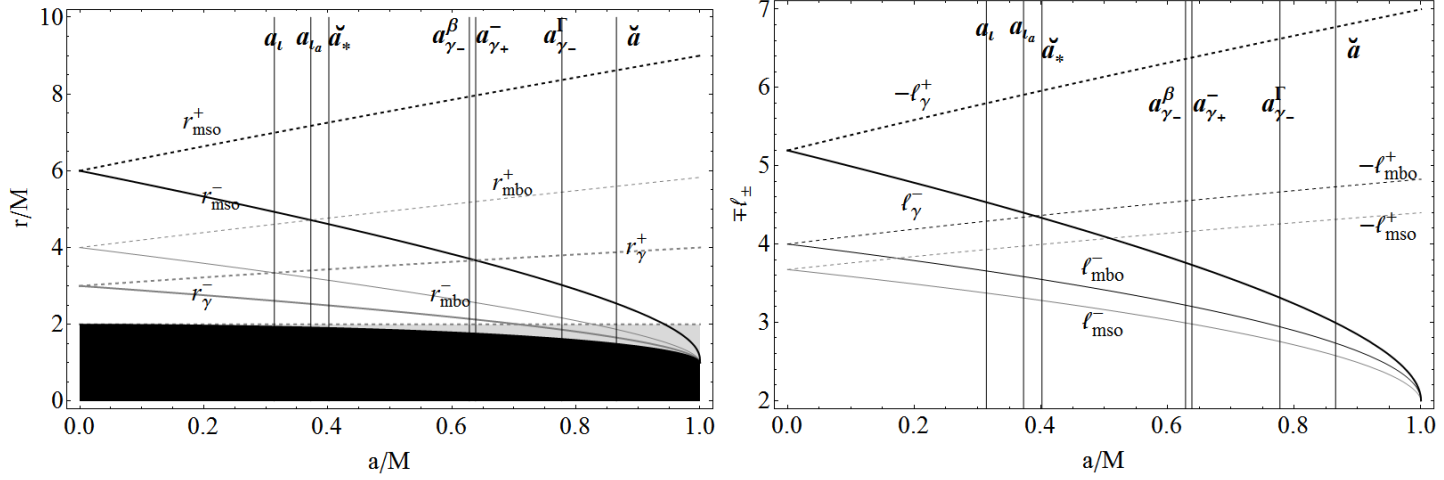


Fig. 2.— Geodesic structure of the Kerr geometry: notable radii $r_{\mathcal{N}} \equiv \{r_{\gamma}^{\pm}, r_{mbo}^{\pm}, r_{mso}^{\pm}\}$ (left panel), and the fluid specific angular momentum $\ell_i^{\pm} = \ell^{\pm}(r_i^{\pm})$ (right panel) where $r_i^{\pm} \in r_{\mathcal{N}}^{\pm}$. Some notable spacetime spin-mass ratios are also plotted. Black region is $r < r_+$, where r_+ is the outer horizon for a Kerr geometry, gray region is $]r_+, r_{\epsilon}^+]$, where $r_{\epsilon}^+ = 2M$ is the outer ergosurface.

sider the orbital region $\Delta r_{crit} \equiv [r_{Max}, r_{min}]$, whose boundaries correspond to the maximum and minimum points of the effective potential respectively. The inner edge of the Boyer surface must be at $r_{in} \in \Delta r_{crit}$, the outer edge is at $r_{out} > r_{min}$. A further matter configuration closest to the black hole is at $r_{in} < r_{max}$. The limiting case of $K_{\pm} = K_{min}^{\pm}$ corresponds to a one-dimensional ring of matter located in r_{min}^{\pm} . The centers r_{cent} of the closed configurations C_{\pm} are located at the minimum points $r_{min} > r_{mso}^{\pm}$ of the effective potential, where the hydrostatic pressure reaches a maximum. The toroidal surfaces are characterized by $K_{\pm} \in [K_{min}^{\pm}, K_{Max}^{\pm}[\subset]K_{mso}^{\pm}, 1[\equiv \mathbf{K0}$ and momentum $\ell_{\pm} \leq \ell_{mso}^{\pm} \leq 0$ respectively. The maximum points of the effective potential r_{Max} correspond to minimum points of the hydrostatic pressure and the P-W points of gravitational and hydrostatic instability. An accretion overflow of matter from the closed, cusped configurations in C_{\pm}^{\pm} (see Fig. (1) towards the attractor can occur from the instability point $r_{\pm}^{\pm} \equiv r_{Max} \in]r_{mbo}^{\pm}, r_{mso}^{\pm}[$, if $K_{Max} \in \mathbf{K0}^{\pm}$ with specific angular momentum $\ell \in]\ell_{mbo}^+, \ell_{mso}^+[\equiv \mathbf{L1}^+$ or $\ell \in]\ell_{mso}^-, \ell_{mbo}^-[\equiv \mathbf{L1}^-$. Otherwise, there can be funnels of material along an open configuration O_{\pm}^{\pm} , proto-jets or for brevity jets, which are limiting topologies for the closed surfaces (Kozłowski et al. 1978; Abramowicz et al. 1978; Sadowski et al. 2015; Lasota et. al. 2015; Lyutikov 2009; Madau 1988; Sikora 1981) with $K_{Max}^{\pm} \geq 1$ ($\mathbf{K1}^{\pm}$), “launched” from the point $r_j^{\pm} \equiv r_{Max} \in]r_{\gamma}^{\pm}, r_{mbo}^{\pm}[$ with specific angular momentum $\ell \in]\ell_{\gamma}^+, \ell_{mbo}^+[\equiv \mathbf{L2}^+$ or $] \ell_{mbo}^-, \ell_{\gamma}^- [\equiv \mathbf{L2}^-$. Equilibrium configurations, with topology C , exist for $\pm \ell_{\mp} > \pm \ell_{mso}^{\mp}$ centered in $r > r_{mso}^{\mp}$ respectively; no maxima of the effective potential exist for $\pm \ell_{\mp} > \ell_{\gamma}^{\pm}$ ($\mathbf{L3}^{\pm}$), and therefore only equilibrium configurations are possible. In general, we mean by the label (i) with $i \in \{1, 2, 3\}$ respectively, any quantity \mathbf{Q} relative to the range of specific angular momentum \mathbf{Li} respectively; for example, C_2^+ indicates a closed regular counter-rotating configuration with specific angular momentum $\ell_2^+ \in \mathbf{L2}^+$. A relevant aspect in this model is that the presence of critical points is regulated mainly by geometric factors (Pugliese&Montani 2015; Pugliese et al. 2012). Following the discussion in Pugliese&Stuchlík (2015) for the unstable modes of a ringed tori, we consider here two types of instabilities emerging in an orbiting macro-structure, leading to a global instability in the ringed disk. Correspondingly, we can distinguish two distinct models of unstable ringed torus $\mathbf{C}^n = \bigcup^n C_i$ made up by n sub-configurations (order n) with degenerate topology : the macro-structure \mathbf{C}_{\odot}^n , with the number $\tau \in [0, n-1]$ (rank of the \mathbf{C}_{\odot}^n torus) of contact points between the boundaries of two consecutive rings, and the macro-structure \mathbf{C}_{\times}^n , with $\tau_{\times} \in [0, n]$ instability P-W points. The number τ_{\times} is

called *rank* of the ringed disk \mathbf{C}_x^n . Finally, we have the macro-structure $\mathbf{C}_\odot^{\times n}$, characterized at last by one contact point that is also an instability point. The P-W local instability affects one or more rings of the ringed disk decomposition, and then it can destabilize the whole ringed disk in the initial \mathbf{C}_x^n topology for collisions of matter between the unstable ring and its consecutive sub-configurations, resulting eventually in a different topology of the entire macro-structure, when the rings are no more separated and a feeding (overlapping) of material occurs. As proved in Pugliese&Stuchlík (2015), if $\tau_x = 1$ and the inner ring \mathbf{C}_x^1 of its decomposition is in accretion, then the whole ringed disk could be globally stable if the outer edge of the accreting ring satisfies proper conditions on the fluid specific angular momentum.

In this article, we consider the existence of several instability points investigating the \mathbf{C}_x^n models with rank $r_x \in [1, n]$, which could also include the open and cusped O_x sub-configurations and the situations where two rings may be in contact or *geometrically correlated* according to constraints settled on their morphology or topology evolution and the geodesic structure of the spacetime. A contact in this model causes collision and penetration of matter, eventually with the feeding of one sub-configuration with material and supply of specific angular momentum of another consecutive ring of the decomposition. This mechanism could possibly end in a change of the ring disk morphology and topology. In the following sections we will face the analysis of the n order decomposition starting from the characterization of the configurations of the order $n = 2$. These can be regarded as seeds for the construction of higher-order macro-configurations generated from this initial couple. We define as *state* or main state a ringed disk of the order $n = 2$ with fixed topology. The notion of state is useful to clarify different aspects of the macro-configuration structure and evolution and to deal with the many different cases occurring even for one couple of rings. In fact, a ringed disk of the order $n = 2$, with fixed equal critical topology could be in $n = 8$ different states according to their rotation and relative position of the centers: $n = 4$ different states, if the rings are ℓ corotating, and $n = 4$ for ℓ countorrotating rings, considering also the relative location of points of minimum pressure. Then, the couple (C_x, O_x) , with different but fixed topology, could be in $n = 16$ different states. For a main state $C_i - ()_x$, considering also the class of magnitude \mathbf{Li} where $i = \{1, 2, 3\}$ for the equilibrium configuration, we need to address $n = 48$ different states. As a result of our analysis we are able to reduce all these possible states to the ones listed in Table (1), whereas details on the restrictions for combinations of different states in ringed disks made up by more than two rings will be presented in future study Pugliese&Stuchlík (2016). We will consider therefore five main states, with at last one critical topology determining the constraints on the state existence and evolution. We will prove that not all the initial and final states are possible and not all the evolutions are actually possible in all spacetimes.

3. States and macro-configuration

To simplify the presentation of the results, we summarize in this section comments on Tables (1), (2) and (3) which schematically introduce some main outcomes of this analysis, whereas we specify the different states for the ℓ corotating couples in Pugliese&Stuchlík (2016) where we extend our investigation to the multiple configurations of the decomposition of the order $n > 2$ providing also evidence of the results and the detailed comments on each case. First we point out that

$$\text{if } ()_i < ()_o, \quad \text{where } \ell_i \ell_o > 0, \quad \text{then } ()_i > ()_o, \quad \text{where } () \in \{C, C_x, O_x\}. \quad (7)$$

For the *ordered* sequences of surface, with the notation $<$ or $>$, we intend the ordered sequence of maximum points of the pressure, or r_{min} , minimum of the effective potential and the configuration centers. In relation to a couple of rings, the terms “internal” (inner) or “external” (outer), will always refer, unless otherwise specified, to the sequence ordered according to the center location. If $C_i < C_j$ then, for $i < j$, C_i is the inner ring, the closest to attractor with respect to C_j , and there is $r_{cent}^i \equiv r_{min}^i < r_{min}^j \equiv r_{cent}^j$. Within these definitions, the rings (C_i, C_{i+1}) and (C_{i-1}, C_i) are *consecutive* as $C_{i-1} < C_i < C_{i+1}$ (Pugliese&Stuchlík 2015). The symbols \succ and \prec refer instead to the sequentiality according to the location of the *minimum* points of the pressure, or r_{Max} , maximum point of the effective potential (in $\mathbf{L1}$ or $\mathbf{L2}$). Thus, for the ℓ corotating sequence there is $()_i < ()_o$ and $()_i \succ ()_o$. Then, the largest is the magnitude of the fluid

specific angular momentum and the largest is the radius of the maximum pressure point and more stretched on the equatorial plane is the configuration, the nearest to the **BH** is the instability point. The situation for a ℓ counterrotating couple with a critical configuration is determined by the two families of the notable radii $r_{\mathcal{N}}^{\pm}$ and by the associated specific angular momenta $\ell_{\mathcal{N}}^{\pm}$ —see Figs.t (2). The discussion of this case is more articulated than the ℓ corotating case. Table (1) summarizes these results. In order to prove these results we

ℓ corotating configurations	ℓ counterrotating configurations
$O_x^i < O_x^o$ and $O_x^i \succ O_x^o$ for $\pm\ell_i^{\mp} < \pm\ell_o^{\mp}$	$O_x^+ \succ O_x^-$ for $a \in \mathbf{A}_{\iota}^{>-}(\mathcal{C})$; $O_x^+ \succ O_x^-$ or $O_x^+ \prec O_x^-$ for $a \in \mathbf{A}_{\iota}^{<-}$
$C_x^i < O_x^o$ and $C_x^i \succ O_x^o$ for $\pm\ell_i^{\mp} < \pm\ell_o^{\mp}$	$C_x^+ \succ O_x^-$
$C_i < O_x^o$ and $O_x^o \prec C_i$ for $\pm\ell_i^{\mp} < \pm\ell_o^{\mp}$	$C_x^- \prec O_x^+$ for $a \in \mathbf{A}_{\iota_a}^{>-}(\mathcal{C}_*)$; $C_x^- \not\prec O_x^+$ for $a \in \mathbf{A}_{\iota_a}^{<-}$
$C_x^a < C_b$ for $\pm\ell_a^{\mp} < \pm\ell_b^{\mp}$ and $\ell_a \in \mathbf{L1}$ $\ell_b \in \mathbf{Li}$	$C_x^- \prec C_x^+$ and $C_x^- \prec C_x^+$
	$C_x^- \prec C_+$ $r_x^- \leq r_{in}^+$ for $a \in \mathbf{A}_{\iota_a}^{<-}$ $-a \in \mathbf{A}_{\iota_a}^{>-}(\mathcal{C}_*)$
	$C_- < C_x^+$ $r_x^+ \geq r_{out}^-$ and $C_x^+ < C_-$ $r_{in}^- \geq r_{out}^+$
	$C_+ < O_x^-$ $r_{out}^+ \not\leq r_J^-$ $r_{in}^+ \geq r_J^-$ (\mathcal{C}) ; $O_x^- < C_+$ $r_{out}^+ \not\leq r_J^-$ $r_{in}^+ \geq r_J^-$ (\mathcal{C})
	$C_- < O_x^+$ $r_{out}^- \leq r_J^+$ $r_{in}^- \geq r_J^+$; $O_x^+ < C_-$ $r_{out}^- \not\leq r_J^+$ $r_{in}^- \geq r_J^+$ (\mathcal{C}_*)

Table 1: Couples with at least one cusped topology. The location of the disk edges is also fixed. The (\mathcal{C}) is for non-correlated configurations, or (\mathcal{C}_*) with particularly restrictive conditions to be satisfied for a correlation to occur—see Pugliese&Stuchlík (2016).

addressed the issue of the location of the matter distribution $(\)_{\pm}$ with respect to notable radii the $r_{\mathcal{N}}$. This is in fact important particularly in the determination of a possible correlation between rings. We discuss the case of ℓ corotating matter, investigating the inclusion³ of $r_{\mathcal{N}}^{\pm} \in (\)_{\pm}$ and of $r_{\mathcal{N}}^{\pm} \in (\)_{\mp}$. It is worth noting here that this investigation actually matches the broader problematic of the location of the inner edge of the disk—see (Krolik&Hawley 2002; Bromley et al. 1998; Abramowicz et al. 2010; Agol&Krolik 2000; Paczyński 2000). Indeed, this investigation will often imply, especially for the inclusion $r_{\mathcal{N}}^{\pm} \in (\)_{\pm}$, a discussion of the location of these radii with respect to the inner margin of the disk, while the location of the outer edge turns to be important especially for the discussion of the $r_{\mathcal{N}}^{\pm} \in (\)_{\mp}$ case. Note that the accretion or proto-jet instability of any sub-configuration is essentially sorted at the inner edge of each ring. Conversely, in the accretion ringed disks, an accretion point or launching point of proto-jet can emerge at any inner margin of any of its rings. Therefore, contrary to the common scenario for a single thick accretion disk, such points of instabilities can emerge in the middle of the macro-structure. Tables (2) and (3) summarize the main results of this analysis. **Table (1)** fixes the five seed states with at least one cusped topology and the possible correlation, establishing also the critical and centers sequentiality, i.e., the relative location of rings of a couple in a particular geometry. We introduce the spin classes:

$$\mathbf{A}_{\iota}^{<-} \equiv [0, a_{\iota}[\quad \text{and} \quad \mathbf{A}_{\iota}^{>-} \equiv [a_{\iota}, M] \quad \text{where} \quad a_{\iota} \equiv 0.3137M : r_{mbo}^- = r_{\gamma}^+, \quad (8)$$

$$\mathbf{A}_{\iota_a}^{<-} \equiv [0, a_{\iota_a}[\quad \text{and} \quad \mathbf{A}_{\iota_a}^{>-} \equiv [a_{\iota_a}, M] \quad \text{where} \quad a_{\iota_a} \equiv 0.372583M : r_{mso}^- = r_{mbo}^+. \quad (9)$$

Some states are uniquely fixed, some states are not possible. The correlation is possible in all corotating couples, according to a proper choice of the “density” K -parameter. The ring separation induced on the ℓ counterrotating couples, due to the attractor rotation, acts in general to forbid or to disadvantage the correlation—see also Pugliese&Stuchlík (2015). This situation is obviously less clear as the spin of the attractor decreases. This would imply that the ℓ counterrotating ring dynamics can be often described as collection of

³The *inclusion* notation, $(\in, \not\in)$ and $\in!$, will be widely used in Tables (2,3). The use of $\bar{r} \in (\)$, for the radius \bar{r} and any surface $(\)$, means that there can be found proper K or ℓ parameters such that this property is satisfied. The symbol $\in!$ is a reinforcement of this inclusion, indicating that this is a necessary relation which is *always* satisfied. The symbol $\not\in$ (meaning non-inclusion) does not generally have any intensifier $!$, which is also used in Table (1), as this analysis is to underline the possibility of inclusion and the condition for this to be satisfied.

Location of the marginally bounded orbits r_{mbo}	
$r_{mbo}^\pm \notin C_3^\pm$;	$r_{mbo}^\pm \notin C_2^\pm$ $r_{mbo}^\pm \in !O_x^{2\pm}$;
$r_{mbo}^\pm \notin C_1^\pm$	$r_{mbo}^\pm \notin C_x^{1\pm}$
Location of the marginally stable orbits r_{mso}	
<i>The configurations $(\)_1^\pm$</i>	
$r_{mso}^\pm \in C_1^\pm$	$r_{mso}^\pm \in !C_x^{1\pm}$;
$\forall \ell_1^\pm \in \mathbf{L1}^\pm$	
<i>The corotating configurations $(\)_2^-$</i>	
$a \in \check{\mathbf{A}}_>$:	$r_{mso}^- \in C_2^-$ $r_{mso}^- \in !O_x^{2-}$
$a \in \check{\mathbf{A}}_<$:	\mathbf{I} $r_{mso}^- \notin C_2^-$ $r_{mso}^- \in !O_x^{2-}$ $\ell_2^- \in]\check{\ell}_-, \ell_\gamma^-[$ $r_{in}^{2-} > r_{mso}^-$;
	\mathbf{II} $r_{mso}^- \in C_2^-$ $r_{mso}^- \in !O_x^{2-}$ $\ell_2^- \in]\ell_{mbo}^-, \check{\ell}_-]$
<i>The counterrotating configurations $(\)_2^+$</i>	
$r_{mso}^+ \in !O_x^{2+}$;	$r_{mso}^+ \in C_2^+$ for $-\ell_2^+ \in]-\ell_{mbo}^+, -\check{\ell}_+]$;
	$r_{mso}^+ \notin C_2^+$ for $-\ell_2^+ \in]-\check{\ell}_+, -\ell_\gamma^+]$
<i>The configurations $(\)_3^\pm$</i>	
$r_{mso}^\pm \notin C_3^\pm$	
$a \in \check{\mathbf{A}}_<$	$r_{mso}^\pm \notin C_3^\pm$;
$a \in \check{\mathbf{A}}_>$	$r_{mso}^\pm \in C_3^\pm$ for $\ell_3^\pm \in]\ell_\gamma^\pm, \check{\ell}_\pm]$, $r_{mso}^\pm \notin C_3^\pm$ for $\ell_3^\pm > \check{\ell}_\pm$
Location of the photon circular orbits r_γ^\pm	
$r_\gamma^\pm \notin (\)_\pm$	

Table 2: Location of the notable radii $r_{\mathcal{N}}^\pm \in (\)_\pm$. This analysis sets location of the inner edge of the disk. In fact we have $r_{in}^{3\pm} > r_{mbo}^\pm$; $r_{in}^{2\pm} > r_{mbo}^\pm$, $r_J^\pm \leq r_{mbo}^\pm$; $r_{in}^{1\pm} > r_{mbo}^\pm$ $r_x^\pm \geq r_{mbo}^\pm$ —see also Pugliese&Stuchlík (2016) for further details on the classes of attractors.

independent (separate) configurations. A more detailed look of Table (1) reveals that in the ℓ counterrotating case the angular momentum is not sufficient to uniquely fix the state and its correlation, but the situation depends on the dimensionless spin of the attractor. In conclusion, the proto jet-accretion correlation is always possible, except in the ℓ counterrotating couples in the geometries of the fastest attractors⁴, $\mathbf{A}_{\iota_a}^>$, with corotating fluid in accretion and counterrotating proto-jet where the point of accretion is always inner with respect to r_J . The case of accretion of counterrotating matter and corotating proto-jet is favored, according to the constraints, in any Kerr geometry, while the case of corotating accretion disk, and counterrotating matter with launching point inner or coincident with the accretion point is favored in the geometries of the slow attractors, $\mathbf{A}_{\iota_a}^<$. A O_x - O_x correlation (i.e. a double-shell of open configurations in contact), is always possible except for the fast attractors, $\mathbf{A}_{\iota_a}^>$, where it is prohibited for an outer counterrotating proto-jet; it is possible for any combination of launching points at low spin geometries $\mathbf{A}_{\iota_a}^<$. The accretion-accretion correlation is possible but with an inner corotating accretion point. The accretion-equilibrium correlation is impossible or not favored for attractors with large spins $\mathbf{A}_{\iota_a}^>$ (being restrictive conditions on the ring parameters) for the counterrotating disk, which must be the outer of the couple with respect to corotating accreting disk. In the case of corotating equilibrium disks a correlation is possible. The proto jet-equilibrium correlation is not possible if there is a corotating jproto-et, and not favored, if the corotating equilibrium disk is outer with respect to the proto-jet configuration. **Table (2)** indicates the location of the orbiting configurations with respect to the ℓ corotating geodesic structure of the Kerr geometry, where there is

$$\check{\mathbf{A}}^< \equiv [0, \check{a}[\quad \text{and} \quad \check{\mathbf{A}}^> \equiv [\check{a}, M] \quad \text{with} \quad \check{a} \equiv 0.969174M : \check{\ell}_- = r_\gamma^- \quad (10)$$

$$\text{and} \quad \check{\ell}_\pm(a/M) : V_{eff}(\check{\ell}_\pm, r_{mso}^\pm) = 1. \quad (11)$$

⁴For *fast* (*slow*) attractors we intend Kerr attractors with high (small) values of the dimensionless spin with respect to some reference values of a/M , fixed considering the geodesic structure of the spacetime in Fig. (2)).

Counterrotating configurations: $r_{\mathcal{N}}^- \in ()_+$

Location of the marginally bounded orbit $r_{mbo}^- \in ()_+$

$$r_{mbo}^- \notin C_3^+;$$

$$a \in \mathbf{A}_{\iota_a}^>: r_{mbo}^- \notin C_2^+, r_{mbo}^- \notin O_x^{2+}$$

$$a \in \mathbf{A}_{\iota_a}^<: r_{mbo}^- \notin C_2^+, r_{mbo}^- \in O_x^{2+}(r_{mbo}^- \succ r_J^{2+}) \quad \text{for} \quad -\ell_+(r_{mbo}^-) \in [-\ell_{mbo}^+, -\ell_+(r_{mbo}^-)]$$

$$r_{mbo}^- \notin C_2^+, r_{mbo}^- \notin O_x^{2+} \quad \text{for} \quad -\ell_+(r_{mbo}^-) \in [-\ell_+(r_{mbo}^-), -\ell_\gamma^+]$$

$$r_{mbo}^- \notin C_1^+ \quad r_{mbo}^- \notin C_x^{1+}$$

Location of the marginally stable orbits $r_{mso}^- \in ()_+$

The configurations $()_1^+$

$$\mathbf{A}_{\iota_a}^>: r_{mso}^- \notin C_1^+, r_{mso}^- \notin C_x^{1+}$$

$$\mathbf{A}_{\iota_a}^<: r_{mso}^- \notin C_x^{1+}, r_{mso}^- \notin C_1^+, \quad \text{for} \quad -\ell_1^+ \in]-\ell_{mso}^+, -\ell_1^+(r_{mso}^-)[$$

$$r_{mso}^- \in C_x^{1+}, r_{mso}^- \notin C_1^+ \quad \text{for} \quad \ell_1^+ = \ell_1^+(r_{mso}^-), \quad r_{in}^{1+} = r_{Max}^{1+} = r_{mso}^- = r_x^+$$

$$r_{mso}^- \in C_x^{1+}, r_{mso}^- \in C_1^+ \quad \text{for} \quad -\ell_1^+ \in [-\ell_1^+(r_{mso}^-), -\ell_{mbo}^+]$$

The configurations $()_2^+$

$$r_{mso}^- \notin C_2^+ \quad \text{for} \quad -\ell_2^+ \in]-\ell_2^+, -\ell_\gamma^+[$$

$$r_{mso}^- \notin C_2^+, r_{mso}^- \notin O_x^{2+} \quad \text{for} \quad a > a_{\gamma_+}^-, r_{mso}^- \notin C_2^+ \quad \text{for} \quad a \in \mathbf{A}_{\iota_a}^>,$$

$$r_{mso}^- \in O_x^{2+} \quad \text{for} \quad a \in]a_{\iota_a}, a_{\gamma_+}^- [\quad \text{and} \quad -\ell_2^+ \in [-\ell_2^+(r_{mso}^-), -\ell_\gamma^+]$$

$$r_{mso}^- \in O_x^{2+} \quad \text{for} \quad a \in \mathbf{A}_{\iota_a}^<, \quad r_{mso}^- \in C_2^+ \quad \text{for} \quad a \in \mathbf{A}_{\iota_a}^< \quad \text{and} \quad -\ell_2^+ \in]-\ell_{mbo}^+, -\ell_{2+}^-].$$

The configurations $()_3^+$

$$r_{mso}^- \notin C_3^+$$

Location of the photon circular orbit r_γ^-

$$r_\gamma^- \notin ()_+$$

Corotating configurations: $r_{\mathcal{N}}^+ \in ()_-$

Location of the marginally stable orbits $r_{mso}^+ \in ()_-$

$$r_{mso}^+ \in C_- \quad \text{for} \quad a \in \check{\mathbf{A}}_*^< \mathbf{L1}^- \cup [\ell_{mbo}^-, \check{\ell}_*^-] \subset \mathbf{L2}^-,$$

$$\text{for } a \in \check{\mathbf{A}}_*^>, \quad \mathbf{L1}^- \cup \mathbf{L2}^- \cup]\ell_\gamma^-, \check{\ell}_*^-] \subset \mathbf{L3}^-$$

Location of the marginally bounded orbits $r_{mbo}^+ \in ()_-$

$$a \in \mathbf{A}_{\iota_a}^<: r_{mbo}^+ \notin C_3^-; \quad r_{mbo}^+ \notin C_2^- \quad \text{for} \quad \ell_2^- \in]\ell_-, \ell_\gamma^- [\quad r_{in}^{2-} > r_{mso}^+ > r_{mbo}^+.$$

$$a > a_{\gamma_-}^\beta: r_{mbo}^+ \in ()_1^-; \quad r_{mbo}^+ \in ()_2^-; \quad r_{mbo}^+ \notin C_3^- \quad \text{for} \quad \ell > \ell_\beta^-; \quad r_{mbo}^+ \in C_3^- \quad \text{for} \quad \ell < \ell_\beta^-$$

$$a < a_{\gamma_-}^\beta: r_{mbo}^+ \in ()_1^-; \quad r_{mbo}^+ \in ()_2^- \quad \text{for} \quad \ell_- < \ell_\beta^-; \quad r_{mbo}^+ \notin ()_2^- \quad \text{for} \quad \ell_- > \ell_\beta^-; \quad r_{mbo}^+ \notin C_3^-$$

Location of the photon circular orbit r_γ^+

$$a \in [0, a_{\gamma_-}^\Gamma]: r_\gamma^+ \in ()_1^- \quad r_\gamma^+ \notin C_3^-; \quad r_\gamma^+ \in ()_2^- \quad \text{for} \quad \ell_- < \ell_\Gamma^-; \quad r_\gamma^+ \notin ()_2^- \quad \text{for} \quad \ell_- > \ell_\Gamma^- \in \mathbf{L2}^-$$

$$a \in]a_{\gamma_-}^\Gamma, M]^*: r_\gamma^+ \in ()_1^- \quad r_\gamma^+ \in ()_2^-; \quad r_\gamma^+ \in ()_3^- \quad \text{for} \quad \ell_- < \ell_\Gamma^- \in \mathbf{L3}^-; \quad r_\gamma^+ \notin ()_3^- \quad \text{for} \quad \ell_- > \ell_\Gamma^- \in \mathbf{L3}^-.$$

Table 3: Location of the notable radii $r_{\mathcal{N}}^\pm \in ()_\mp$. This analysis sets location of the edge of the disk.

We analyzed the inclusion relations $r_{\mathcal{N}}^\pm \in ()_\pm$ setting, particularly, the location of the ring inner edge. The marginally bound orbit is never included in any equilibrium or accretion topology. This implies that the disk inner edge must be always external to this, whereas the launching point of proto-jet must be internal. The marginally stable orbit must be always included in any unstable ring and it can also be included in the equilibrium C_1^\pm configuration with a density lower then the critical one ($K < K_{Max}$). The crossing of the marginally stable orbit does not lead, by itself, to the P-W instability. The situation at higher spin is much more complex and depends generally on two classes of attractors and the direction of rotation of the fluid with respect to these. For corotating disks in $\mathbf{L2}$, whose unstable mode is a proto-jet, orbiting fast attractors, $\check{\mathbf{A}}_>$, the marginally stable orbit can be included in their equilibrium configurations ($r_{in} < r_{mso}^-$ depending on the K -parameter). At lower spins, $\check{\mathbf{A}}_<$, this cannot occur (as $r_{in} > r_{mso}^-$) but for lower specific angular

momentum. For the counterrotating configurations the occurrence of $r_{mso}^+ \in C_2^+$ does not depend directly on the attractors but again for high magnitudes of specific angular momentum, the marginally stable orbit is not included in the disk, the limiting specific angular momenta being however function of the dimensionless a/M (Pugliese&Stuchlík 2016). At higher specific angular momentum magnitudes, **L3**, for which there is no unstable mode, there has to be $r_{in}^+ > r_{mso}^+$ for any attractor. Whereas $r_{in}^- > r_{mso}^-$ for $\check{\mathbf{A}}_<$, while in $\check{\mathbf{A}}_>$ the marginally stable orbit may be included in C_3^- for low specific angular momentum. **Table (3)** indicates the location of each ring with respect to the ℓ counterrotating geodesic structure of the Kerr geometry, examining the inclusion $r_{\mathcal{N}}^\mp \in (\)_\pm$, where there is

$$\check{\mathbf{A}}_< \equiv [0, \check{a}_*] \text{ and } \check{\mathbf{A}}_> \equiv [\check{a}_*, M] \text{ where } \check{a}_* \equiv 0.401642M : \check{\ell}_* = \ell_\gamma^-, \text{ and } \check{\ell}_* : V_{eff}(\check{\ell}_*, r_{mso}^+) = 1, \quad (12)$$

$$a_{\gamma-}^\beta \equiv 0.628201M : \ell_\beta^- = \ell_\gamma^- \text{ where } \ell_\beta^- : V_{eff}(\ell_\beta^-, r_{mbo}^+) < 1, \quad (13)$$

$$a_{\gamma-}^\Gamma \equiv 0.777271M : \ell_\Gamma^- = \ell_\gamma^- \text{ where } \ell_\Gamma^- : V_{eff}(\ell_\Gamma^-, r_\gamma^+) = 1, \quad (14)$$

$$a_{\gamma+}^- \equiv 0.638285M : r_\gamma^+ = r_{mso}^-, \quad (15)$$

$$\check{\ell}_{2+}^- : V_{eff}(\ell_2^+, r_{mso}^-) = 1 \text{ and } \check{\ell}_2^- = \check{\ell}_- \in \mathbf{L2}. \quad (16)$$

This analysis provides also more restrictive constraints for the location of the inner edge of a ring, providing also information on the ring outer margins.

The study of the inclusion of the ring margins with respect to the ℓ counterrotating geodesic structure of the Kerr geometry is essential to establish a possible correlation between the ℓ counterrotating fluids and related evolution. Several results of this analysis were in fact used in Table (1)–see also Pugliese&Stuchlík (2016). We focus first on the counterrotating fluids. According to Table (3), the proto-jet launching point can be internal to r_{mbo}^- for sufficiently low spin, $\mathbf{A}_\ell^<$, and low specific angular momenta in magnitude only. Then the launching point must be external to r_{mso}^- in the geometries $a > a_{\gamma+}^-$. It must be internal for slower attractors, and in $\mathbf{A}_{\iota_a}^>$ for sufficiently high angular momentum magnitudes. It must be internal for low spins, $\mathbf{A}_{\iota_a}^<$, and for all values of specific angular momentum.

We focus now on the inner edge of the counterrotating disk in equilibrium or in accretion with respect to r_{mso} . At this point the analysis is more complicated because the double geodesic structure includes crossing points between the elements of $r_{\mathcal{N}}^\pm$, therefore the situation strongly depends on the geometric properties of the Kerr spacetimes. We show that the ratio ℓ/a must have specific characteristics for an instability to emerge. Concerning the accretion points, the most significant aspect perhaps is that the point of accretion must be internal with respect to r_{mso}^+ –Table (2), but ring must not include r_{mso}^- in the $\mathbf{A}_{\iota_a}^>$ geometries–Table (3). Viceversa, we have to take into account if the fluid is orbiting $\mathbf{A}_{\iota_a}^<$ attractors with sufficiently high specific momentum magnitude. On the other hand, focusing on the C_1^+ disk, this can contain the orbit r_{mso}^+ without being unstable, but it cannot contain r_{mbo}^- for any **BH** spin; it cannot contain r_{mso}^- for $\mathbf{A}_{\iota_a}^>$ class, it can be included viceversa for sufficiently slower spin attractors, $\mathbf{A}_{\iota_a}^<$ and large magnitude of the specific angular momentum. The inner edge of the equilibrium C_2^+ configurations can be internal to r_{mso}^- only for slow attractors and specific angular momentum with a sufficiently low magnitude.

The more articulated situation concerns the corotating disks and their location with respect to the counterrotating geodesic structure. For this analysis it was necessary to thoroughly analyze the situation of the outer edge of the closed topology, as there are in fact $r_a^- < r_a^+$ for $r_a \in r_{\mathcal{N}}$. Here we deal the case $r_a^+ \in [r_{in}^-, r_{out}^-]$. We start with the inclusion of the photon orbit r_γ^+ which is the innermost radius in the structure determined by $r_{\mathcal{N}}^+$. There are two classes of attractors. For $a < a_{\gamma-}^\Gamma$, radius r_γ^+ can always be in $(\)_1^-$, but never in C_3^- , while for $r_\gamma^+ \in (\)_2^-$ a sufficiently low angular momentum is required. For faster attractors, there is in general always $r_\gamma^+ \in (\)_1^-$ and $(\)_2^-$, but in C_3^- a sufficiently low specific angular momentum is required. The orbit $r_{mbo}^+ \in C_1^-$, but is never in C_3^- for $a \in \mathbf{A}_{\iota_a}^<$, in this class it is in C_2^- only for sufficiently low specific angular momentum. At larger a/M it is always $r_{mbo}^+ \in C_2^-$, while there is $r_{mbo}^+ \in C_3^-$ only for the lower ℓ_3^- . The situation is in general more articulated for C_2^- and C_3^- and it depends on $a_{\gamma-}^\beta$: for large a/M there is $r_{mbo}^+ \in (\)_2^-$ only for large specific momenta, for large spin there can be always $r_{mbo}^+ \in (\)_2^-$

while it is in C_3^- only for low enough momenta. The marginally stable orbit $r_{mso}^+ > r_{mso}^-$ can always be in $(\)_1^-$ for the geometries $\check{A}_*^<$, and in $(\)_2^-$ only for low specific angular momentum. For large spin attractors instead it can be included in $(\)_1^-$ and $(\)_2^-$, and in $(\)_3^-$ only for lower spins. Further discussion on methods and applications of the instabilities, details of each individual state and the precise definition of the limits of angular momentum will be presented in Pugliese&Stuchlík (2016) where it is also shown how composition of more rings in macro configuration is in many cases strongly constrained and evolution limited.

4. Conclusions and Future Perspectives

We addressed instabilities emerging in the ringed accretion disks introduced in Pugliese&Stuchlík (2015), considering in particular conditions for the emergence of unstable phases for each ring according to the P-W mechanism and the condition for the destabilization of macro-configuration after a rings collision. First, we proved that the existence of a couple of rings is strongly constrained with respect to the relative location of the configurations in the couple, the ring instability, the relative rotation, and the rotation with respect to the attractor and, in the case of ℓ counterrotating rings, the dimensionless spin on the central Kerr black hole. Considering ringed disks with at last one critical point, we established the orbital and critical rings sequentiality, the location of instability points, and the inner and outer margins of each ring, as well as the emergence of possible contact points between two sub-configurations (correlation), which can lead to collision in a C_\odot^n unstable macro-configuration—Table (1). Some results of this investigation naturally apply to the case of only one accretion disk, which can be considered as the simplest ringed disk of the order $n = 1$. The analysis, in the framework of the ringed disks, in particular th clarifies significant and widely debated issue of the location of the inner (and outer) edge of an accretion disk, where in general emergence of P-W instability occurs. We constrained the location of the inner and outer edges of each toroidal ring according to its specific angular momentum, and the geodesics structure of the Kerr spacetime, and the K -parameter involved in the ring density definition—Tables (2,3). This study was in fact relevant in the determination of rings relative location and the recognition of correlation. Properties of the ringed disk, reflected in Tables (1,2,3), could be used to identify the background geometry in one of the particular class of attractors considered here. Highlighting the possibility that there may be structures formed by more then one accretion torus orbiting around a Kerr attractor we believe that present work could have significance in the high-energy astrophysics, playing possibly a significant role in some of already observed phenomena, namely in terms of interaction and dynamics of several rings of the macro-configuration. The unstable modes and the ring collisions could lead to several phenomena eventually involving the attractor itself, like for example the runaway instability (Abramowicz et al. 1983, 1998; Rezzolla et al. 2003; Font&Daigne 2002a; Hamersky&Karas 2013; Korobkin et al. 2013). From methodological point of view, by considering a purely hydrodynamic model with a constant specific angular momentum, this analysis captures some significant aspects of the basic geometric properties of the extended matter configurations, considered in some way as the relativistic generalization of geodesic structure to the extended objects with pressure gradients, relevant for this structure. Thus, the considerations traced here could be applicable also for more general models where the specific angular momentum is not constant along the disk Lei et al. (2008). A further generalization of this work should consider the role of the magnetic fields in the macro-structures.

The authors acknowledge the institutional support of the Faculty of Philosophy and Science of the Silesian University of Opava. Z.S. acknowledges the Albert Einstein Center for Gravitation and Astrophysics supported by the Czech Science Foundation grant No. 14-37086G. D. P. acknowledges also the Accademia Nazionale dei Lincei for support during 2015 (within the Royal Society fellowship program), the Junior GACR grant of the Czech Science Foundation No:16-03564Y, and useful discussions with Prof. J. Miller, Prof. M. A. Abramowicz, Prof. V. Karas at RagTime17 workshop.

REFERENCES

Abramowicz, M. A. 1971, Acta. Astron., 21, 81

Abramowicz , M. A. 2008, arXiv:astro-ph/0812.3924

Abramowicz, M. A., Calvani, M. & Nobili, L. 1983, *Nature*, 302, 597–599

Abramowicz, M. A. & Fragile, P.C. 2013, *Living Rev. Relativity*, 16, 1

Abramowicz, M.A., Jaroszynski, M., Kato, S., et al. 2010, *A&A*, 521, A15

Abramowicz, M.A., Jaroszyński, M. & Sikora, M. 1978, *A&A*, 63, 221

Abramowicz, M.A., Karas, V. & Lanza, A. 1998, *A&A*, 331, 1143

Abramowicz, M.A., & Sharp, N.A. 1983, *Ap&SS*, 96, 431

Agol, E. & Krolik, J. 2000, *ApJ*, 528, 161

Alig, C., Schartmann, M., Burkert, A., Dolag, K. 2013, *ApJ*, 771, 2, 119

Allen, S. W., Dunn, R.J.H., Fabian, A.C., et al 2006, *MNRAS*, 1, 372, 21

Boyer, R.H. 1965, *Proc. Camb. Phil. Soc.*, 61, 527

Bromley, B. C., Miller, W. A. & Pariev, V. I. 1998, *Nature*, 391, 54, 756

Carmona-Loaiza, J.M., Colpi, M., Dotti, M. & Valdarnini R. 2015, *MNRAS*, 453, 1608

Chakrabarti, S. K. 1990, *MNRAS*, 245, 747

Chakrabarti, S. K. 1991, *MNRAS*, 250, 7

Chen, Y., Zhang, X., Zhang, H. et al 2015, *Ap&SS*, 357, 2, 100

Coughlin, E. R. & Begelman, M. C. 2014, *ApJ*, 781, 82

Cremaschini, C. Kovar J., Slaný P., Stuchlík Z. & Karas V. 2013, *ApJS*, 209, 15

Dogan, S., Nixon, C., King, A., & Price, D. J. 2015 *MNRAS*, 449, 2, 1251

Dunhill, A., Alexander, R., Nixon C., & King A. 2014, *MNRAS*, 445, 3, 2285

Dyda, S., Lovelace, R.V.E., Ustyugova, G.V., Romanova, M.M. & Koldoba, A.V. 2015, *MNRAS*, 446, 613

Fender, R. & Munoz-Darias, T. 2015, arXiv:1505.03526

Ferreira, J. & Casse, F. 2004, *ApJ*, 601, L139

Font, J. A. & Daigne, F. 2002a, *MNRAS*, 334, 383

Font, J. A. & Daigne, F. 2002b, *ApJ*, 581, L23–L26

Fragile, P.C., Wilson, J. & Rodriguez, M. 2012, *MNRAS*, 424, 524

Frank, J., King, A., Raine, D., *Accretion Power in Astrophysics*, Cambridge University Press-2002

Gafton, E., Tejeda, E., Guillochon, J., Korobkin, O. & Rosswog, S. 2015, *MNRAS*, 449, 1, 771

Ghisellini, G., Tavecchio, F., Maraschi, L., et al. 2014 *Nature*, 515, 376

Hamersky, J. & Karas, V. 2013, *A&A*, 32, 555

Hohlfeld, R. G. & Lovelace, R.V.E. 2014, *Journal of Physics:Conference Series*, 640, 1

- Igumenshchev, I. V. & Abramowicz, M. A. 2000, *ApJS*, 130, 463
- Karas, V. & Sochora, V., 2010, *ApJ*, 725, 2, 1507–1515
- King, A. R. & Pringle, J. E. 2006, *MNRAS*, 373, L93
- King, A. R. & Pringle, J. E. 2007, *MNRAS*, 377, L25
- Korobkin, O., Abdikamalov, E., Stergioulas, N., et al. 2013, *MNRAS*, 431, 1, 354
- Kovar, J., Stuchlík, Z. & Karas, V. 2008, *Class. Quant. Grav.*, 25, 095011
- Kozłowski, M., Jaroszynski, M. & Abramowicz, M. A. 1978, *A&A* 63, 1–2, 209–220.
- Krolik, J.H. & Hawley, J.F. 2002, *ApJ*, 573, 754
- Lasota, J.-P., Vieira, R.S.S., Sadowski, A., Narayan, R. & Abramowicz M. A. 2015, arXiv:1510.09152
- Lei, Q., Abramowicz, M. A., Fragile, P. C., Horak, J., Machida, M. & Straub O. 2008, *A&A.*, 498, 471
- Lovelace, R. V. E. & Chou, T. 1996, *ApJ*, 468, L25
- Lovelace, R. V.E., Romanova, M. M., Lii, P. & Dyda, S. 2014, *Computational Astrophysics and Cosmology*, 1-3
- Lyutikov, M. 2009, *MNRAS*, 396, 3, 1545–1552
- Madau, P. 1988, *ApJ*, 1, 327, 116–127
- Maitra, D., Markoff, S., Brocksopp C., et al. 2009, *MNRAS*, 398, 4, 1638–1650
- Maraschi, L. & Tavecchio, F. 2003, *ApJ*, 593, 667
- Marscher, A. P., Jorstad, S. G., Gomez, J. L., et al 2002, *Nature*, 417, 625–627
- McKinney, J.C., Tchekhovskoy, A., & Blandford, R.D. 2013, *Science*, 339, 49
- Miller, J.M., Pooley, G.G., Fabian, A.C., et al. 2012, *ApJ*, 757, 11
- Miller, J. M., Kaastra, J. S., Coleman Miller, M., et al 2015, *Nature*, 526, 542–545
- Nixon, C.J. & King A. R. 2012, *MNRAS*, 421, 12011208
- Nixon, C.J., King, A.R., & Price D.J. 2012a, *MNRAS*, 422, 25472552
- Nixon, C., King, A. & Price, D. 2013, *MNRAS*, 434, 1946
- Nixon, C., King, A., Price, D., & Frank, J. 2012b *ApJ*, 757, L24
- Nixon, C. J. & King, A. R. & Pringle, J. E. 2011, *MNRAS*, 417, 1, L66-L69,
- Okuda T., Teresi, V., Toscano E. & Molteni, D. 2005, *MNRAS*, 357, 295
- Paczynski, B. 1980, *Acta Astron.*, 30, 4
- Paczynski, B. 2000, astro-ph/0004129.
- Pugliese, D. & Kroon, J.A.V. 2012, *Gen. Rel. Grav.*, 44, 2785
- Pugliese, D. & Montani, G. 2015, *Phys. Rev. D*, 91, 083011
- Pugliese, D., Montani, G., & Bernardini, M. G. 2012, *MNRAS*, 428, 952

- Pugliese, D. & Quevedo, H. 2015, Eur. Phys. J. C, 75, 5, 234
- Pugliese, D., Quevedo, H. & Ruffini, R. 2011, Phys. Rev. D, 84, 044030
- Pugliese, D., Quevedo, H. & Ruffini, R. 2013, Phys. Rev. D, 88, 2, 024042
- Pugliese, D. & Stuchlík, Z. 2015, ApJS, 221, 2, 25
- Pugliese, D. & Stuchlík, Z., *in preparation*
- Rezzolla, L., Zanotti, O. & Font, J.A. 2003 A&A, 412, 603
- Sadowski, A., Lasota, J.P., Abramowicz, M.A. & Narayan, R. 2015, arXiv:1510.08845
- Sadowski, A. & Narayan, R. 2005, arXiv:1503.00654
- Sbarrato, T., Padovani, P. & Ghisellini, G. 2014, MNRAS, 445, 1, 81.
- Slaný, P. & Stuchlík, Z. 2005 Class. Quantum Gravity, 22, 3623
- Sikora, M. 1981, MNRAS, 196, 257
- Sochora, V., Karas, V., Svoboda, J. & Dovciak, M. 2011, MNRAS, 418, 276–283
- Stuchlík, Z. 2005, Mod. Phys. Lett., A, 20, 561
- Stuchlík, Z. & Kolos, M. 2016, Eur. Phys. J. C, 76, 1, 32
- Stuchlík, Z., Pugliese, D., Schee J. & Kucakova, H. 2015, Eur. Phys. J. C, 75, 9, 451
- Stuchlík, Z. & Schee, J. 2012, Class. Quant. Grav., 29, 6
- Stuchlík, Z. & Schee, J. 2010, Class. Quant. Grav., 27, 215017
- Stuchlík, Z., Slaný, P. & Kovar, J. 2009, Class. Quant. Grav., 26, 215013
- Volonteri, M., Haardt, F. & Madau, P. 2003, ApJ, 582 559
- Yu, X., Zhang, X., Zhang, H., Xiong, D., et al. 2015, Ap&SS, 357, 14
- Zanotti O. & Pugliese D. 2015, Gen. Rel. Grav., 47, 4, 44
- Zhang J., Xue Z.W., He J.J., Liang E.W. & Zhang S.N. 2015, ApJ, 807, 1, 51